

## DAWN MANEUVER DESIGN PERFORMANCE AT VESTA

**D.W. Parcher<sup>\*</sup>, M. Abrahamson<sup>\*</sup>, A. Ardito<sup>†</sup>, D. Han<sup>\*</sup>, R.J. Haw<sup>\*</sup>,  
B.M. Kennedy<sup>\*</sup>, N. Mastrodemos<sup>\*</sup>, S. Nandi<sup>\*</sup>, R.S. Park<sup>\*</sup>, B.P. Rush<sup>\*</sup>, B.A.  
Smith<sup>\*</sup>, J.C. Smith<sup>\*</sup>, A.T. Vaughan<sup>\*</sup>, and G.J. Whiffen<sup>\*</sup>**

The Dawn spacecraft orbited the asteroid Vesta from July 16, 2011 to September 5, 2012, successfully accomplishing the four planned science orbits and two planned rotational characterization orbits. The lowest-altitude science orbit lasted four months, with 20 planned orbit maintenance maneuvers. Navigation results from Vesta demonstrate that the navigation plan was sufficient to achieve orbit delivery accuracy requirements. This paper compares the flown Dawn trajectory against the planned trajectory and expected maneuver dispersions. Understanding the effectiveness of the Vesta maneuver design plan is a key component of planning for operations at Ceres, the next destination for the Dawn mission.

### INTRODUCTION

The first destination for the Dawn mission was Vesta, the second most massive asteroid in the main asteroid belt. Dawn traveled to Vesta for the purpose of gaining a better understanding of Vesta's composition, interior structure, and formation<sup>1,2,3</sup>. The spacecraft orbited Vesta from July 16, 2011 to September 5, 2012, observing the asteroid from a variety of orbits during that time in addition to maneuvering between those orbits. After studying Vesta for almost 14 months<sup>4,5,6,7,8,9</sup>, and having completed all planned operations at Vesta, the spacecraft departed to travel to its next target, Ceres.

The Dawn spacecraft relies on solar-electric, low-thrust ion propulsion for all orbital maneuvers as well as interplanetary cruise. Between launch and arrival at Vesta, the spacecraft's ion propulsion system accomplished 6.69 km/s  $\Delta V$ , propelling the spacecraft past a Mars flyby in February of 2009 to capture at Vesta on July 16, 2011. At Vesta, the spacecraft performed 350 m/s of additional  $\Delta V$ , transferring between Vesta observation orbits as high as 6,000 km and as low as 172 km altitude.

The Vesta mission included 6 targeted near-polar orbits. The first, and highest, orbit was not an official science orbit, but rather was classified as a rotational characterization orbit due to the limited scope of the observations. At 5,500 km semi-major axis, the rotational characterization orbit provided high altitude observations of Vesta. The spacecraft spent only 5.3 days in this orbit, less than one 7-day orbital period, before diving deeper into Vesta's gravity field.

---

<sup>\*</sup> Members of the Engineering Staff, Guidance Navigation and Control Section, Jet Propulsion Laboratory, California Institute of Technology, 4800 Oak Grove Drive, Pasadena, California 91109-8099.

<sup>†</sup> Former member of the Engineering Staff, Guidance Navigation and Control Section, Jet Propulsion Laboratory. Currently a member of the Engineering staff at ARPSOFT s.r.l., via bolsena 40, Rome, Italy, 00123.

The Dawn spacecraft travelled to a total of four science orbits. In order, they are Survey (3,000 km orbital radius), the High Altitude Mapping Orbit known as HAMO (950 km orbital radius), the Low Altitude Mapping Orbit known as LAMO (475 km orbital radius), and the second High Altitude Mapping Orbit known as HAMO-2 (950 km orbital radius). After the four science orbits, the mission included one more rotational characterization orbit at (5,550 km semi-major axis) where the spacecraft spent only 4.5 days out of the 7.2 day orbital period before departing toward Ceres. These 6 targeted orbits at Vesta are shown in Figure 1.

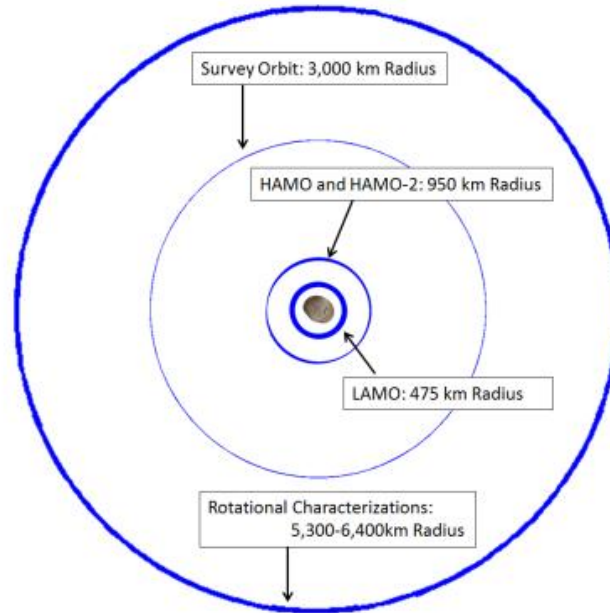


**Figure 1 - Targeted Orbits at Vesta**

This paper compares expected delivery dispersions<sup>10</sup> to each of the four science orbits against the actual delivery accuracies. Additional discussions include an analysis of navigation accuracy during science orbit transfers, and a comparison of the maneuver execution error models to the maneuver execution errors deduced from the final maneuver designs flown.

## PROCESS

The navigation paradigm at Vesta<sup>10,11,12,13</sup> involved building reference trajectories to take the spacecraft from each science orbit to the next. These reference trajectories were flown in smaller segments, each of which was targeted back to the reference trajectory\*. Each of these segments is referred to as a maneuver. In this way, as the spacecraft deviated from the designed reference trajectory, it was periodically corrected back toward the reference trajectory, limiting a buildup of navigation errors. Reference trajectories and maneuvers were designed and optimized using Mystic, a Static Dynamic Optimal Control algorithm developed by Gregory Whiffen<sup>14,15,16</sup>.

---

\* Flying back to the reference trajectory was a paradigm used for orbit-to-orbit transfers, but not on approach to Vesta. The approach trajectory<sup>11</sup> targeted the pre-Survey rotational characterization orbit in addition to Survey in a series of 5 maneuvers. Each approach maneuver design also included redesigning all subsequent maneuvers to eventually achieve the orbital parameters for those two orbits. In this way, the approach trajectory did not include a reference trajectory, but rather changed the entire approach with each maneuver.

Figure 2 shows an example reference trajectory timeline. The timeline consists of 4 maneuvers (green), each targeting back to the reference trajectory. The targeted states along the reference trajectory are called Waypoints, and are indicated at the end of each maneuver. Waypoints are nothing more than states on the reference trajectory that the maneuvers target. Each maneuver is designed prior to execution (purple). In the case of the second and third maneuvers in Figure 2, the maneuvers are designed during the execution of the prior maneuver. The first and fourth maneuvers are designed during a science orbit (blue) or other planned coasting (red). Each maneuver is designed following a radiometric tracking pass (data cutoff) used by the Dawn Orbit Determination (OD) team to determine the spacecraft state and estimate Vesta’s physical parameters. The spacecraft state at the data cutoff is mapped forward to the start of the maneuver. This OD prediction of the spacecraft state at the next Waypoint is corrupted by any thrusting between the data cutoff and the start of the maneuver – as occurs for the second and third maneuvers in Figure 2. Accurate OD Waypoint (maneuver start) prediction is a key component of successful navigation.

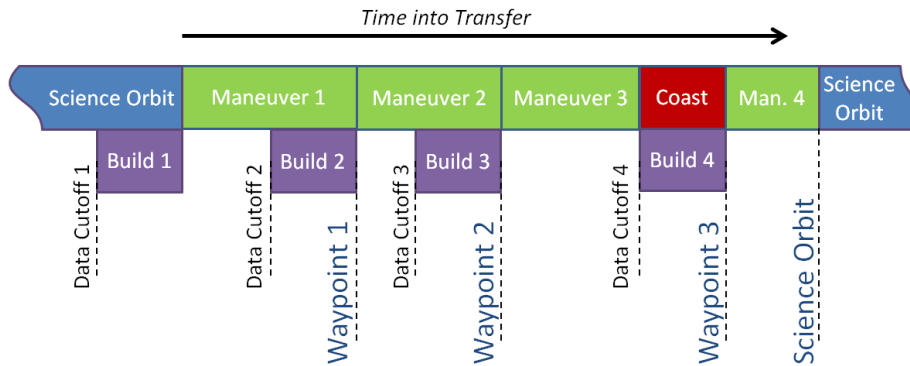


**Figure 2 - Science Orbit Transfer Concept (Example Timeline Shown for Survey to HAMO)**

At Vesta, maneuvers were primarily used to transfer between science orbits. Only one of the Vesta science orbits, LAMO, required maneuvers during the orbit itself. LAMO was the most dynamic of the science orbits, and required periodic orbit maintenance maneuvers to return the spacecraft to the designed orbit. This was done not only to protect the science observation plan from rapidly growing navigation errors, but also to prevent the spacecraft from wandering away from the orbital stability characteristics inherent in the selected LAMO reference<sup>12</sup>.

Orbit transfer maneuvers and LAMO Orbit Maintenance Maneuvers (OMM) were simulated using Veil<sup>10</sup>, a Monte Carlo trajectory optimization program utilizing Mystic. Veil was used to re-optimize low-thrust trajectories to the science orbit targets while simulating errors in orbit determination, low-thrust maneuver execution, attitude control thrusting, and the physical parameters of Vesta. Uncertainties for maneuver execution errors were developed by the Dawn Attitude Control and OD teams based on spacecraft performance during the cruise to Vesta as well as models of expected spacecraft behavior at Vesta. The error models and resulting delivery dispersions determined by the Veil Monte Carlo analysis represent the expected maneuver accuracy during Vesta operations. These simulated maneuver dispersions are compared to the OD reconstruction<sup>17</sup> of the spacecraft trajectory at Vesta to produce the results presented in this paper.

Each of these low-thrust maneuvers required changing the orientation of the spacecraft throughout the maneuver to achieve the designed thrust direction profile\*. Determination of the

---

\* Each LAMO maintenance maneuver was designed in a fixed inertial direction but still required thruster gimbaling to counteract gravity gradient torque from Vesta.

angular maneuver execution errors was accomplished by comparing the designed thrust profile against spacecraft telemetry of Dawn attitude and thruster gimbal position throughout each maneuver. The results presented in this paper include the spacecraft telemetry-based determination of angular thrust direction error for each of the maneuvers executed and a comparison of those errors against the Monte Carlo simulation maneuver execution error models.

Figure 3 shows the thrust profile for a maneuver during the first transfer, between Survey and HAMO, and illustrates the significant variation in thrust direction over the course of a single maneuver. The Monte Carlo models used to simulate maneuver execution error modeled short-term errors, errors that occur on short timescale compared to the length of a maneuver. By contrast, the Dawn OD team estimated persistent maneuver direction and magnitude biases that occurred across multiple maneuvers for the purpose of accounting for those biases in future designs. Short-term errors were not estimated for two reasons: first, because it was not necessary to estimate short-term errors to provide the desired orbit determination accuracy, and second, estimating short-term errors was found to be ineffective due to the lack of observability of such errors. The lack of observability was due in part to the infrequent radiometric tracking compared to the time scale of thrust direction changes. As a result, the OD estimation of direction and magnitude errors cannot be directly compared against the maneuver execution models used to develop the navigation plan. The Dawn OD estimation of the time-varying thrust direction and magnitude errors are discussed further in Reference 17.

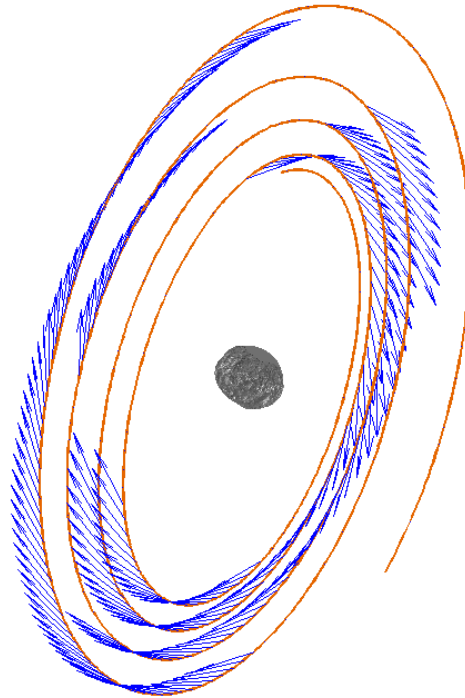


**Figure 3 – Single example maneuver during the transfer from Survey to the High Altitude Mapping Orbit at Vesta. Thrust times and directions are represented with blue arrows. Maneuver Ends at Waypoint 1.**

The comparisons of the planned execution accuracy against achieved execution accuracy presented in this paper may prove beneficial for future low-thrust missions in developing navigation plans for orbital operations, and will be leveraged for development of the Dawn navigation plan for Ceres operations.

## RESULTS

The expected delivery dispersions during each of the science orbit transfers and throughout LAMO are compared against actual delivery accuracies based on orbit determination reconstruction of the spacecraft trajectory. The Vesta approach trajectory, which targeted both the pre-Survey rotational characterization orbit and Survey itself, is not included in this discussion. This is done for brevity and to allow focus on maneuver execution error models, which were not the primary focus of approach\*. Also, a discussion of the trajectory targeting the final rotational characterization and the Vesta departure trajectory is not included. This was also done for brevity and to allow focus on the more challenging orbit-to-orbit transfers.

The first orbit transfer discussed is the Survey to High Altitude Mapping Orbit (Survey to HAMO) transfer, followed by the High Altitude Mapping Orbit to Low Altitude Mapping Orbit (HAMO to LAMO) transfer. Next is a discussion of the LAMO Orbit Maintenance Maneuver performance, followed by the Low Altitude Mapping Orbit to second High Altitude Mapping Orbit (LAMO to HAMO-2) transfer.

### Survey to High Altitude Mapping Orbit Transfer

The Survey to High Altitude Mapping Orbit (Survey to HAMO)<sup>11</sup> transfer reference trajectory contained 4 planned maneuver designs targeting Waypoints on the reference trajectory. The expected delivery to each of the Waypoints as determined by Monte Carlo Analysis<sup>10</sup> is shown in Table 1 alongside the reconstructed delivery error. The first two columns respectively represent the expected OD prediction accuracy of the spacecraft state at each Waypoint and the actual OD prediction accuracy based on the transfer reconstruction. These columns illustrate the accuracy with which the start state of each maneuver was predicted from the data cutoff (see Build periods in Figure 2). The OD prediction of a Waypoint ultimately affects the delivery accuracy of the corresponding maneuver. The final two columns in Table 1 contain the expected maneuver delivery error and the actual maneuver delivery error based on the transfer reconstruction, respectively. These columns illustrate how well each maneuver was able to deliver to its intended target. For each listed OD prediction, the delivery accuracy from the maneuver designed with that OD solution is found on the next row. The table shows that the majority of deliveries were sub-sigma, especially the Waypoint prediction accuracy.

**Table 1. Survey to HAMO Modeled Waypoint Delivery Dispersion and Actual Delivery**

Survey to HAMO Waypoint	Modeled Waypoint prediction Uncertainty (km, $1\sigma$ )	Distance between OD prediction and Waypoint (km) <sup>†</sup>	Modeled Delivery Dispersion (km) from Reference Trajectory ( $1\sigma$ )	Actual Delivery Distance (km) from Reference Trajectory <sup>†</sup>
Survey End	8.0	0.6	--	--
Waypoint 1	20.8	2.3	52.8	55.5
Waypoint 2	20.8	2.4	60.1	36.0
Waypoint 3	0.9	0.3	61.7	38.6
HAMO	--	--	2.8	0.16
<sup>†</sup> Based on orbit determination reconstruction, with uncertainty below 200 m and 2 cm/s $1\sigma$				

\* The approach trajectory to Vesta contained only mildly varying thrust directions and small execution errors. Greater focus was placed on Vesta's physical characteristics such as pole orientation and gravity.

Figure 4 shows the evolution of the reconstructed spacecraft position and velocity during the executed maneuvers compared to the 4 maneuver designs targeting each of the Survey to HAMO Waypoints. The initial deviation for each of the trajectory arcs shown is non-zero because the orbit determination solution used to design that maneuver occurred days prior to the start of the maneuver execution, often before thrusting from the previous maneuver had completed. The initial deviation in Figure 4, also shown as distance from OD prediction in Table 1, is a measure of the OD prediction accuracy of the start state for that maneuver\*. Note, for example, that the Maneuver targeting Waypoint 1 starts at a position error of less than 1 km. This is because the OD solution used to design the maneuver occurred during Survey, and no thrusting occurred between that OD solution and the beginning of the transfer to HAMO. A similar effect occurs for the final maneuver, which also contained no thrusting between the OD solution used to design the maneuver and the execution of the maneuver itself. This was by design, to improve delivery accuracy to HAMO<sup>10</sup>. Meanwhile, the Maneuvers targeting Waypoints 2 and 3 relied on OD solutions based on data that occurred prior to the end of thrusting of the previous maneuver. This degraded the prediction of the Waypoint state, but was done to reduce transfer time<sup>10</sup>.

Deviations from the maneuver design trajectory increase throughout the maneuver execution due to compounding errors. This is seen the least during the final maneuver targeting HAMO due to the short maneuver duration. Whereas the previous maneuvers contained significant amounts of deterministic thrusting required to transfer from Survey altitude to HAMO altitude, the final maneuver contained only statistical thrusting, and amounted primarily to a phase adjustment. In order, the 4 designed maneuvers accomplished 25.8, 26.7, 12.7 and 0.18 m/s  $\Delta V$ . See Figure 3 for an illustration of the maneuver targeting Waypoint 1.

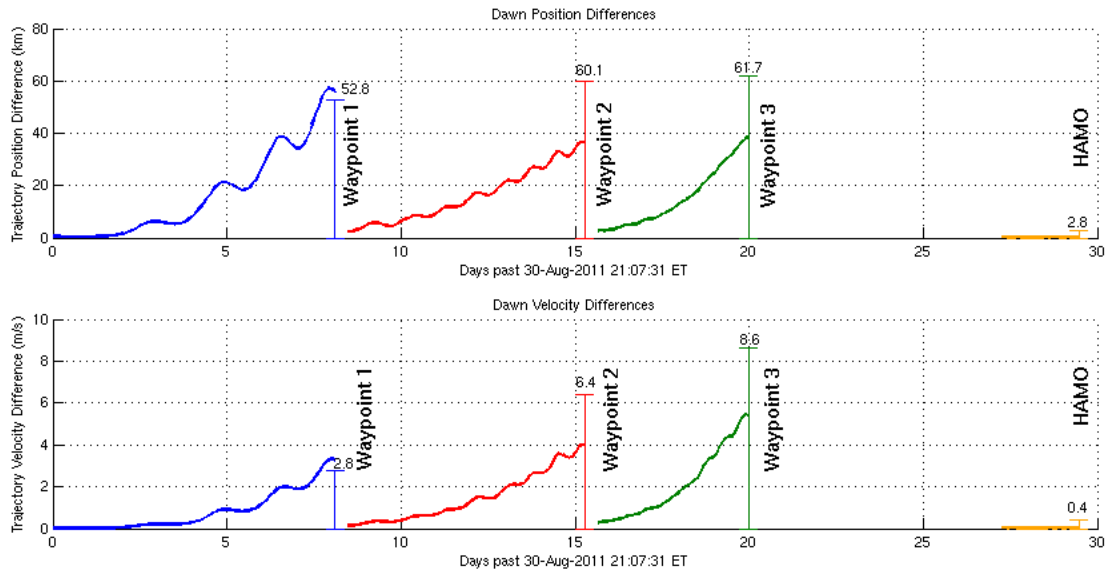


**Figure 4 - Survey to HAMO Maneuver Design Trajectories versus Reconstructed Transfer Trajectory**

\* The values shown in Table 1 represent the OD reconstruction compared to the reference trajectory. The values shown in Figure 4 represent OD reconstruction compared to the designed maneuvers - in principle a different comparison. However, these comparisons are the same at each Waypoint because the designed maneuvers and the reference trajectory are, by design, identical at the Waypoints.

Another interesting comparison is the difference between the reference trajectory designed to be flown, and the reconstructed trajectory actually flown, shown in Figure 5. The difference shown demonstrates how far the spacecraft deviated from the reference trajectory between Waypoints. In some cases, large deviations occurred due to attitude control requirements on the Waypoint targeting maneuvers. The over 200 km excursion near the end of the transfer was the result of the delivery error to Waypoint 3 being allowed to propagate for a week. A maneuver correcting this error was planned to execute at 23 days in Figure 5, but failed to execute.

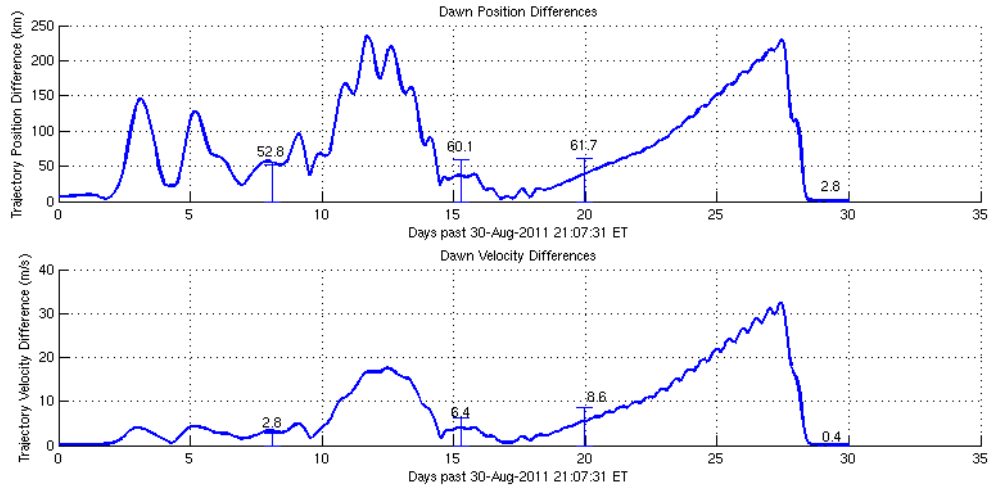


**Figure 5 - Survey to HAMO Reference Trajectory versus Reconstructed Transfer Trajectory**

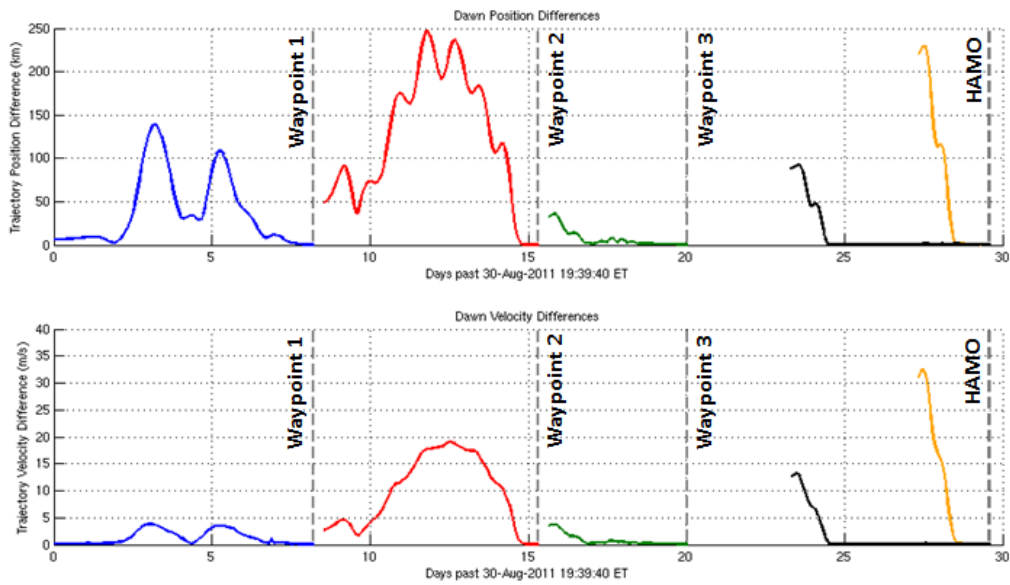


**Figure 6 - Survey to HAMO Maneuver Design Trajectories versus Reference Trajectory**

Figure 6 contains the differences between each of the 4 designed maneuvers and the reference trajectory. This chart illustrates both how accurately each Waypoint was achieved near the start of each maneuver (the beginning of each of the arcs), as well as how far each maneuver intentional-

ly carried the spacecraft away from the reference trajectory before returning to the reference trajectory at the next waypoint. The largest deviation occurs between Waypoints 1 and 2, where attitude control constraints were particularly challenging. This maneuver was the first to employ *thrust direction optimization* to satisfy attitude control requirements<sup>18</sup>, and sent the spacecraft far from the reference before arriving at the next Waypoint. Optimizing the thrust direction during the maneuver rather than optimizing final mass was one of the primary methods used to control the thrust profile to avoid difficult combinations of spacecraft attitude and attitude rate.

Note that there are two maneuvers targeting HAMO. The first maneuver, occurring 23 days into the transfer in Figure 6, was designed but failed to execute. At that point, the spacecraft energy was already largely consistent with HAMO\*, but orbit phase had drifted significantly from the planned HAMO. The second attempt at this phase adjustment was successfully executed starting on day 27 in Figure 6.

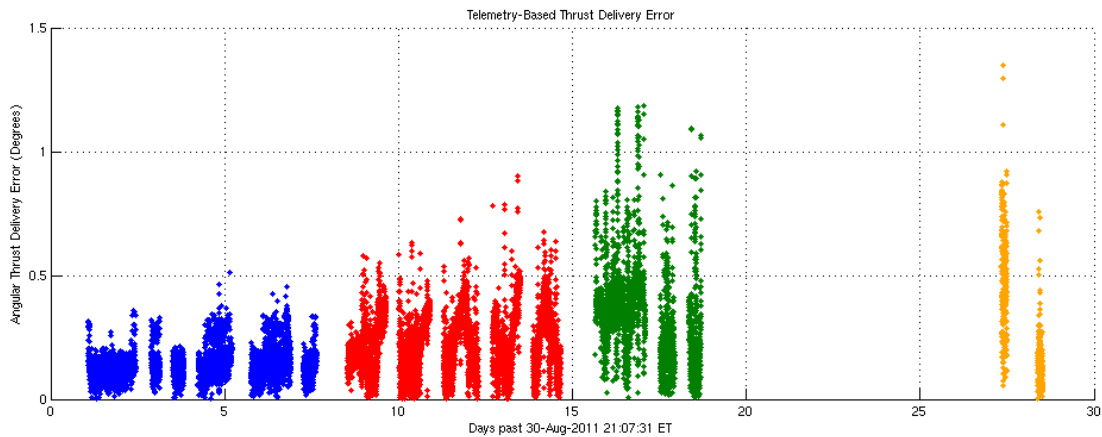


**Figure 7 - Survey to HAMO Spacecraft Telemetry-Based Attitude Control Thrust Delivery Errors**

Finally, Figure 7 includes a calculation of angular thrust delivery error due to attitude control implementation of the designed maneuvers. These errors are calculated from spacecraft telemetry taken during the maneuver. As such, Figure 7 does not include an estimation of the total maneuver execution pointing error, but captures the best understanding of execution pointing error during the transfer. The Dawn orbit determination team estimated persistent maneuver direction and magnitude biases that occurred across multiple maneuvers for the purpose of accounting for those biases in future designs rather than determining short term errors<sup>17</sup>. As a result, the orbit determination estimation of direction and magnitude errors cannot be directly compared against the maneuver execution models used to develop the navigation plan.

The Veil Monte Carlo analysis used to develop the navigation plan for this transfer<sup>10</sup> assumed that the spacecraft would regularly suffer up to 1.75 degrees of pointing error and occasionally more than 8 degrees. By comparison, errors in Figure 7 rarely exceed 1 degree.

---

\* Following the delivery from Waypoint 3, the orbital period was under 2 minutes in error from the HAMO target of 12.3 hours. However, the error in orbital period would have been sufficient to cause significant problems to the HAMO groundtrack and would have required the final maneuver, even had the phase error not been present.



## High Altitude Mapping Orbit to Low Altitude Mapping Orbit Transfer

The High Altitude Mapping Orbit to Low Altitude Mapping Orbit (HAMO to LAMO)<sup>11</sup> transfer reference trajectory contained 10 planned maneuver designs targeting back to the reference trajectory. The expected delivery to each of these Waypoints as determined by Monte Carlo Analysis is shown in Table 2 alongside the reconstructed delivery error. The table shows that the majority of Waypoint deliveries were sub-sigma.

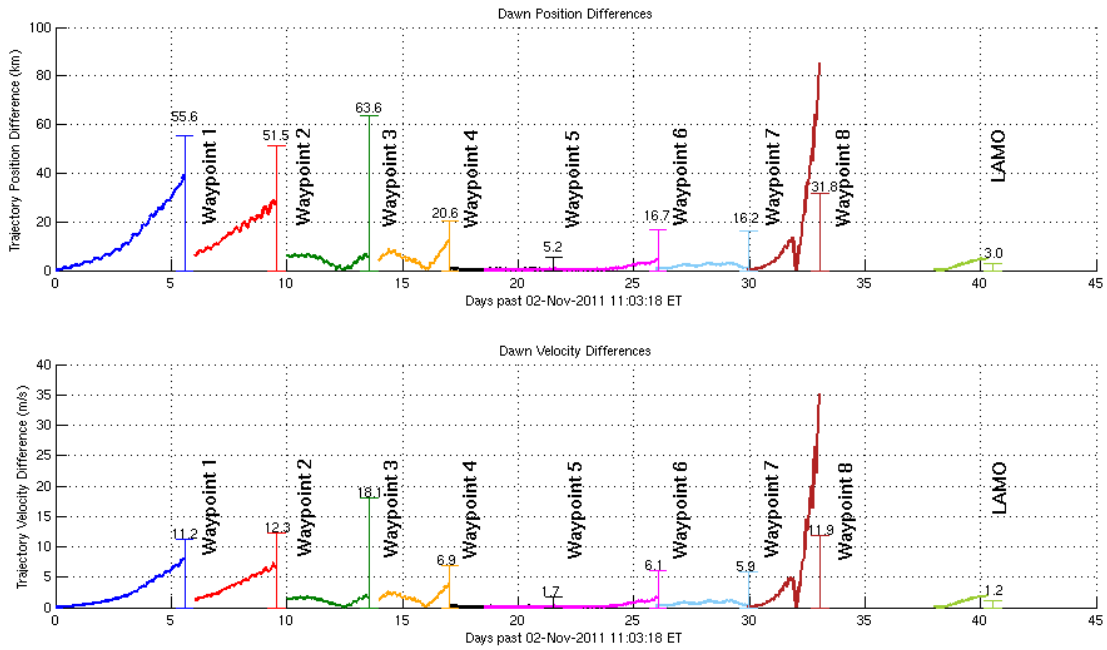
The only delivery errors that were larger than  $1\sigma$  occurred at Waypoints 8 and 9, where the spacecraft failed to fully execute the planned maneuver targeting Waypoint 8, and did not perform a recovery maneuver until after Waypoint 9. The failed maneuver resulted in poor delivery to Waypoints 8 and 9 and disrupted OD prediction of the start state of Waypoint 8, invalidating statistical comparison with the modeled uncertainty. From the remaining results, it is apparent that the Monte Carlo analysis for the HAMO to LAMO transfer resulted in conservative estimates of the delivery statistics to the Waypoints.

**Table 2. HAMO to LAMO Modeled Waypoint Delivery Dispersion and Actual Delivery**

HAMO to LAMO Waypoint	Modeled Waypoint prediction Uncertainty (km, $1\sigma$ )	Distance between OD prediction and Waypoint (km)*	Modeled Delivery Dispersion (km) from Reference Trajectory ( $1\sigma$ )	Actual Delivery Distance (km) from Reference Trajectory*
HAMO End	0.8	0.05	--	--
Waypoint 1	22.8	6.1	55.6	39.4
Waypoint 2	20.4	5.9	51.5	27.7
Waypoint 3	19.2	4.3	63.6	5.6
Waypoint 4	7.3	0.5	20.6	12.2
Waypoint 5	2.0	0.05	5.2	0.2
Waypoint 6	2.4	0.6	16.7	4.4
Waypoint 7	14.2	0.4	16.2	1.1
Waypoint 8	15.7	96.2**	31.8	83.7 <sup>†</sup>
Waypoint 9	1.9	0.5	50.3	234.7 <sup>†</sup>
LAMO	--	--	3.0	0.6

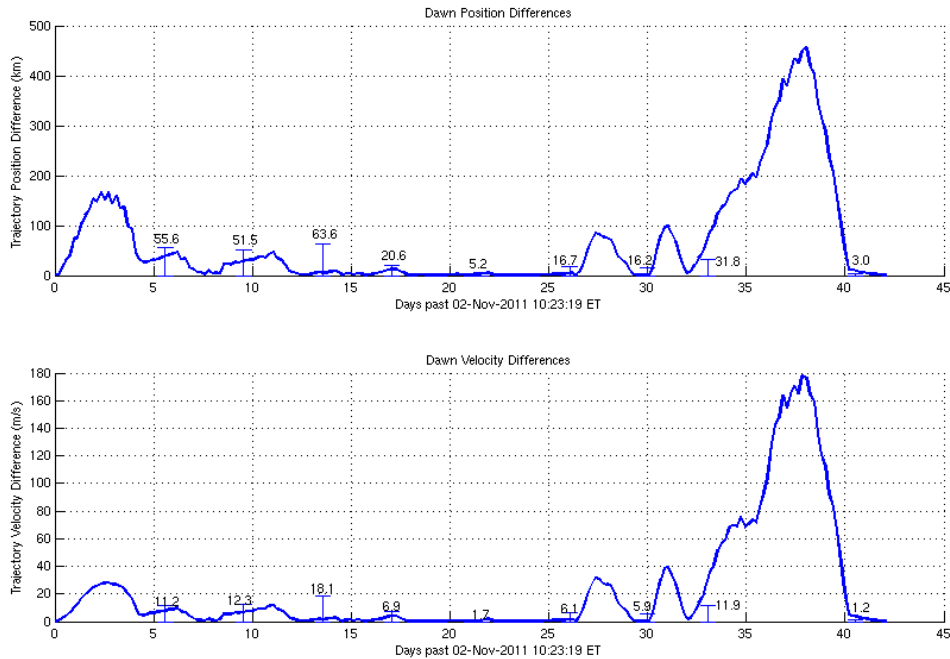
\* Based on orbit determination reconstruction, with uncertainty below 50 m and 1 cm/s  $1\sigma$ .  
<sup>†</sup> The maneuver targeting Waypoint 8 did not completely execute, affecting the OD prediction of the Waypoint 8 state, as well as Waypoint 8 and 9 deliveries. A recovery maneuver occurred after the Waypoint 9 epoch.

Figure 8 shows the evolution of the reconstructed spacecraft position and velocity during the executed maneuvers compared to the 10 planned maneuver designs targeting each of the HAMO to LAMO Waypoints. As with Survey to HAMO, the initial deviation for each of the maneuvers shown in Figure 8 illustrates the OD prediction accuracy of the start state for that maneuver, also shown in Table 2. At approximately day 32 in Figure 8, the maneuver targeting Waypoint 8 prematurely ended, causing the sharp deviation from the designed trajectory. This occurred after the maneuver targeting Waypoint 9 was designed, but before it executed, resulting in the maneuver being aborted. The final maneuver in Figure 8 recovered from the failure and placed the spacecraft in LAMO. The high degree of accuracy for the final maneuver is due to the fact that it was a small maneuver, accomplishing only 2.4 m/s  $\Delta V$ .



**Figure 8 - HAMO to LAMO Maneuver Design Trajectories versus Reconstructed Transfer Trajectory**

The difference between the reference trajectory designed to be flown and the reconstructed trajectory actually flown is shown in Figure 9. The differences shown illustrate how far the spacecraft deviated from the reference trajectory between Waypoints. Between day 32 and day 40, the deviation was caused by the incomplete maneuver targeting Waypoint 8.



**Figure 9 - HAMO to LAMO Reference Trajectory versus Reconstructed Transfer Trajectory**

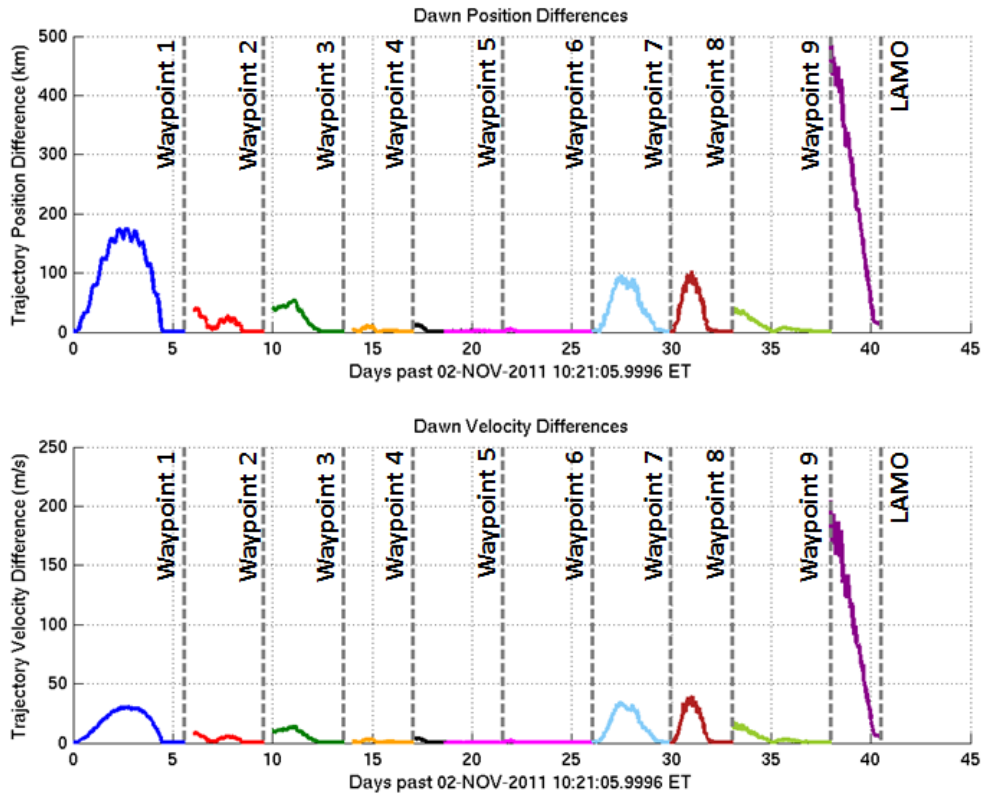


**Figure 10 - HAMO to LAMO Maneuver Design Trajectories versus Reference Trajectory**

Figure 10 shows the difference between each of the 10 designed maneuvers and the reference trajectory. This chart illustrates both how accurately each Waypoint was achieved near the start of each maneuver, as well as how far each maneuver intentionally carried the spacecraft away from the reference trajectory in order to achieve the next Waypoint or to satisfy attitude control constraints. The largest intentional deviations occur prior to Waypoint 1 and between Waypoints 6 and 8. It is interesting to note that the largest intentional deviation from the reference for HAMO to LAMO is smaller than the largest deviation from Survey to HAMO. This can be attributed to the HAMO to LAMO reference trajectory having more favorable nominal thrust directions. Attitude control constraints prevent the spacecraft from maneuvering quickly while the thrust vector is near the Sun/Anti-Sun line. As a lesson from the Survey to HAMO experience, the HAMO to LAMO reference trajectory was designed with this constraint in consideration. This particular HAMO to LAMO reference trajectory was selected over other candidates partly because it avoided deterministic thrusting near the Sun/Anti-Sun line<sup>19</sup>.

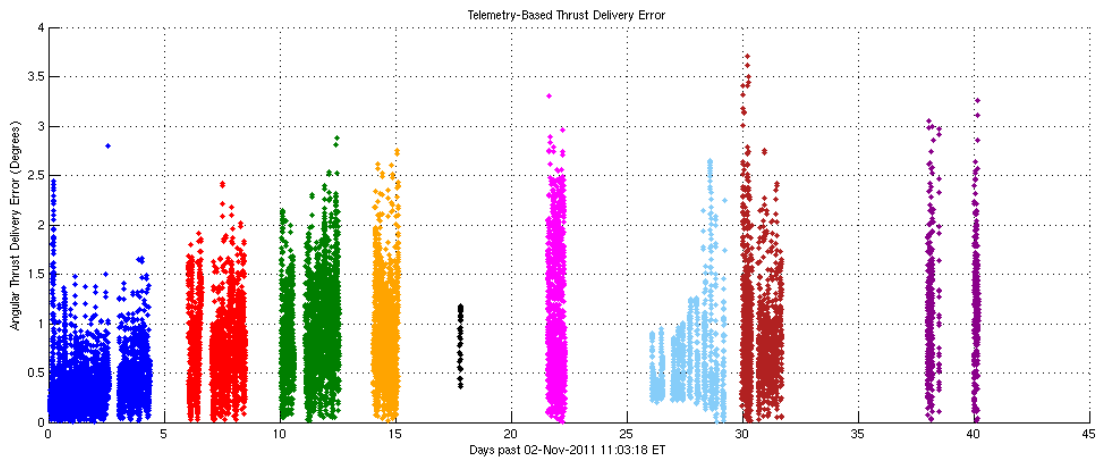


**Figure 11 - HAMO to LAMO Spacecraft Telemetry-Based Attitude Control Thrust Delivery Errors**

Finally, Figure 11 includes the spacecraft telemetry-based determination of angular thrust delivery error for each of the designed maneuvers during the transfer. The Veil Monte Carlo analysis used to develop the navigation plan for this transfer<sup>10</sup> assumed that the spacecraft would suffer more than 1 degree of pointing error at all times, more than 3 degrees of pointing error for just over 10% of the each maneuver, and occasional deviations of more than 10 degrees. By comparison, 76% of the values shown in Figure 11 are less than 1 degree, only 0.15% exceed 3 degrees, and none exceed 4 degrees.

### Low Altitude Mapping Orbit

The Low Altitude Mapping Orbit (LAMO) contained 10 planned Orbit Maintenance Maneuver pairs<sup>12</sup> targeting back to the reference orbit. Each OMM pair consisted of one maneuver designed to change the spacecraft state such that it began drifting toward the reference trajectory, and a second maneuver a week later designed to remove the drift so that the spacecraft would stay near the reference. These pairs of maneuvers were designed simultaneously to work together to return the spacecraft to the reference LAMO. The expected delivery to each of the Waypoints is shown in Table 3 alongside the reconstructed delivery error. Of the 10 planned maneuver pairs, 2 were cancelled as a result of a particularly accurate delivery from the previous maneuver. Delivery is not shown for cancelled maneuvers (Waypoints 5 and 9) in Table 3 due to the fact that cancellation is not taken into account in the statistical results. The spacecraft was also unable to execute the maneuvers targeting Waypoints 3 and 6. Recovery maneuvers targeted the following Waypoint in both cases.

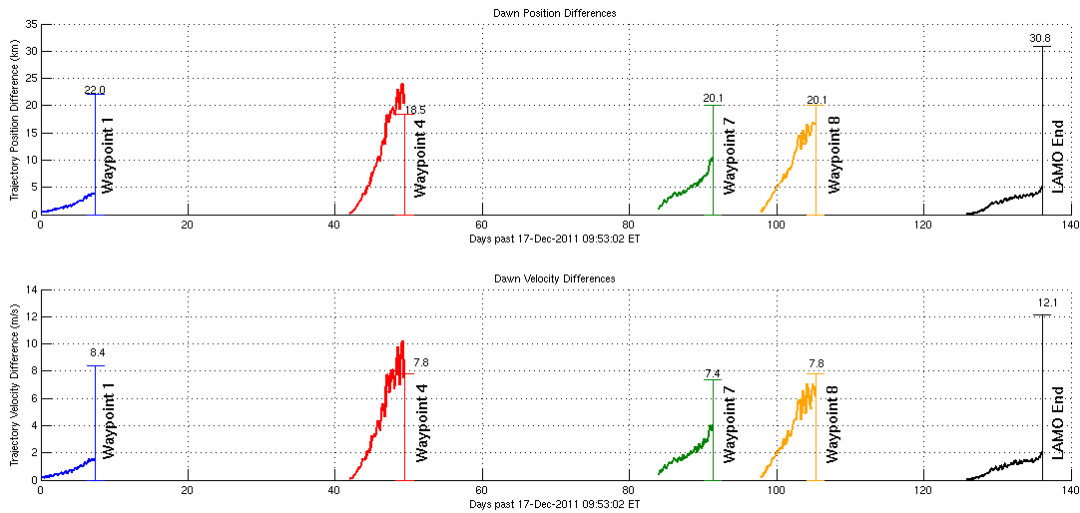
Table 3 shows that all but one of the deliveries for executed maneuvers were sub-sigma. As a result, it is apparent that the Monte Carlo analysis for the LAMO resulted in conservative estimates of the delivery statistics to the Waypoints.

**Table 3. Modeled LAMO Orbit Maintenance Maneuver Delivery Dispersion and Actual Delivery**

LAMO Waypoint	Modeled Waypoint prediction Uncertainty (km, $1\sigma$ )	Distance between OD prediction and Waypoint (km)*	Modeled Delivery Dispersion (km) from Reference Trajectory ( $1\sigma$ )	Actual Delivery Distance (km) from Reference Trajectory*
LAMO Start	3.73	0.9	--	--
Waypoint 1	3.76	0.7	22.0	3.9
Waypoint 2	4.38	0.6	20.7	--
Waypoint 3	4.01	0.2	23.0	84.5 <sup>†</sup>
Waypoint 4	3.84	0.1	18.5	22.0
Waypoint 5	4.23	2.8	18.9	--
Waypoint 6	4.24	0.9	20.4	305.3 <sup>†</sup>
Waypoint 7	3.96	0.4	20.1	10.6
Waypoint 8	3.61	1.8	20.1	16.5
Waypoint 9	4.00	0.06	20.0	--
LAMO End	--	--	30.7	5.2

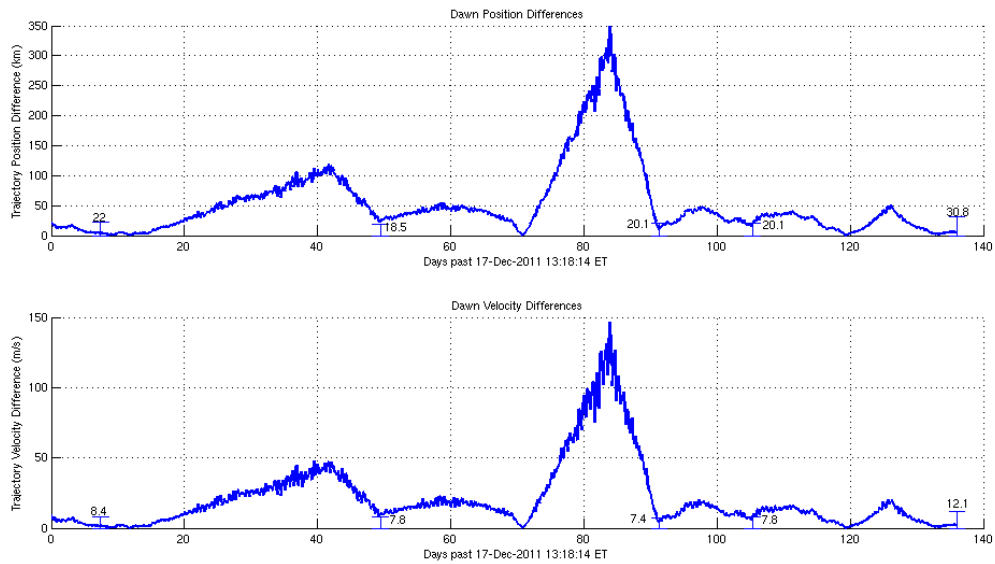
\* Based on orbit determination reconstruction, with uncertainty below 10 m and 5 mm/s  $1\sigma$ .  
<sup>†</sup> The maneuvers targeting Waypoints 3 and 6 did not execute, affecting the delivery. The recovery maneuvers targeted Waypoints 4 and 7 respectively.

Figure 12 shows the evolution of the reconstructed spacecraft position and velocity during the executed maneuvers compared to the maneuver designs targeting each of the LAMO Waypoints. Throughout LAMO, OD prediction accuracy and maneuver delivery accuracy generally improved due to refinements in knowledge of Vesta’s gravity field, and a better understanding and prediction of reaction wheel momentum desaturation maneuvers.



**Figure 12 - LAMO Orbit Maintenance Maneuver Design Trajectories versus Reconstructed Science Orbit Trajectory**

The difference between the reference trajectory and the reconstructed trajectory actually flown is shown in Figure 13. For LAMO, attitude control constraints were not a significant issue as the average total  $\Delta V$  for each pair of maneuvers was low (0.34 m/s). Maneuvers were short, and in inertially fixed directions. The large 350 km excursion toward the middle of LAMO was caused by cancellation of maneuvers determined to be unnecessary for LAMO safety<sup>6</sup> and science return.



**Figure 13 - LAMO Reference Orbit versus Reconstructed Science Orbit Trajectory**

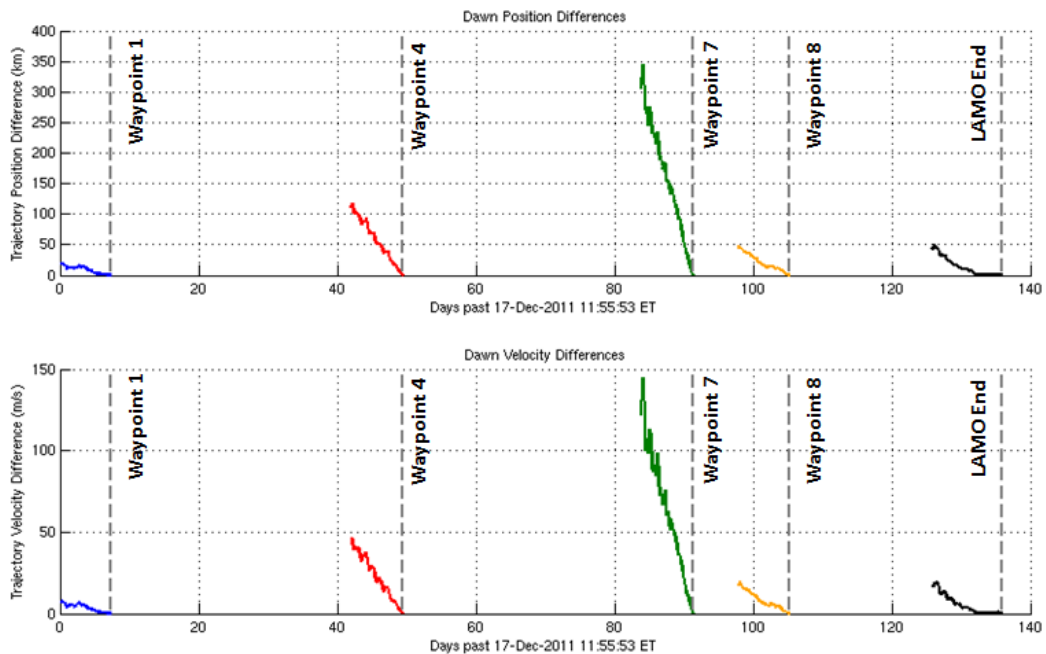


**Figure 14 - LAMO Orbit Maintenance Maneuver Design Trajectories versus Reference Orbit**

Figure 14 illustrates the difference between each of the 5 designed maneuvers and the reference orbit. This chart illustrates the planned drift back to the reference trajectory for each of the maneuvers. In each case, the drift starts with the first maneuver of the pair, moves toward the reference for one week, and ends with a second maneuver removing the drift and placing the spacecraft back on the reference. The largest starting distance from the reference trajectory occurs for the maneuver targeting Waypoint 7, a distance which was the result of the failure to execute a maneuver targeting Waypoint 6.

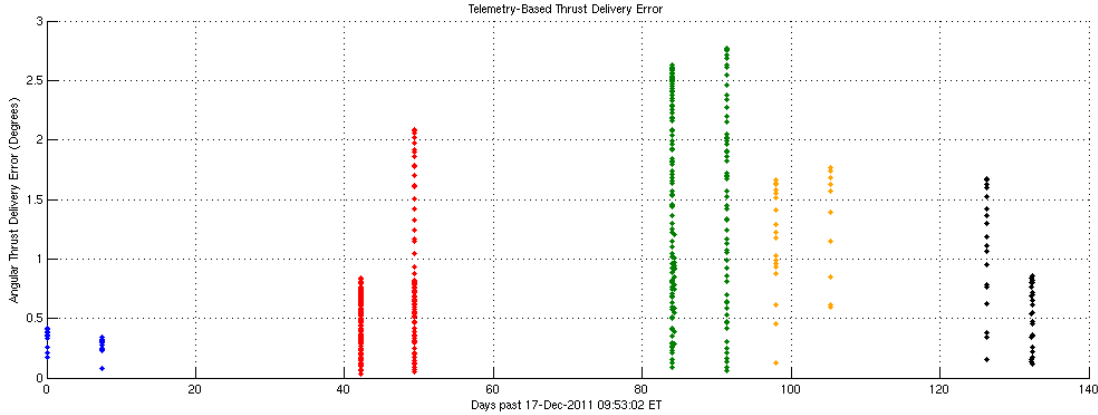


**Figure 15 - LAMO Orbit Maintenance Spacecraft Telemetry-Based Attitude Control Thrust Delivery Errors**

Finally, Figure 15 includes the spacecraft telemetry-based determination of angular thrust delivery error for each of the designed maneuvers during LAMO. The Veil Monte Carlo analysis used to develop the navigation plan for LAMO<sup>10</sup> assumed that the spacecraft would suffer more than 1 degree of pointing error at all times, more than 3 degrees of pointing error for just over 10% of the each maneuver, and occasional deviations of more than 10 degrees. By comparison, 65% of the values shown in Figure 15 are less than 1 degree, and none exceed 3 degrees.

This result is partially due to the way LAMO OMMs were designed. The Monte Carlo analysis assumed that the maneuvers would have a time-varying direction and would occasionally require aggressive attitude control during thrusting which would result in large thrust delivery errors. In practice, it was far easier to design maneuvers in inertially fixed directions. When OMMs were optimized with time-varying thrust directions, the result was often wild thrust direction changes in pursuit of very small gains in the optimization objective function. In many cases, this would have resulted in maneuvers that could not have been performed with the Dawn attitude control system. Not only did optimizing each maneuver with a single direction make satisfying attitude control constraints significantly easier, it improved the accuracy of each OMM\*, and at insignificant cost in propellant.

---

\* Despite each LAMO OMM being in a single inertially fixed direction, significant angular thrust delivery errors result from the use of thrust gimbaling to counteract gravity gradient torque on the spacecraft. This effect is most pronounced at low altitudes deep within Vesta's gravity well.

## Low Altitude Mapping Orbit to Second High Altitude Mapping Orbit Transfer

The Low Altitude Mapping Orbit to Second High Altitude Mapping Orbit (LAMO to HAMO-2)<sup>11</sup> transfer reference trajectory contained 11 planned maneuver designs targeting back to the reference trajectory. The expected delivery to each of these Waypoints as determined by Monte Carlo Analysis<sup>10</sup> is shown in Table 4 alongside the reconstructed delivery error. The table shows that the majority of deliveries were sub-sigma. As a result, it is apparent that the Monte Carlo analysis for the LAMO to HAMO-2 transfer resulted in conservative estimates of the delivery statistics to the Waypoints.

**Table 4. LAMO to HAMO-2 Modeled Waypoint Delivery Dispersion and Actual Delivery**

LAMO to HAMO-2 Waypoint	Modeled Waypoint prediction Uncertainty (km, $1\sigma$ )	Distance between OD prediction and Waypoint (km)*	Modeled Delivery Dispersion (km) from Reference Trajectory ( $1\sigma$ )	Actual Delivery Distance (km) from Reference Trajectory*
LAMO End	4.1	0.9	--	--
Waypoint 1	15.9	1.8	13.5	21.3
Waypoint 2	1.7	0.1	22.0	13.7
Waypoint 3	17.2	1.9	11.2	5.6
Waypoint 4	6.3	2.0	22.0	5.6
Waypoint 5	17.4	0.3	30.5	4.4
Waypoint 6	17.5	4.5	52.6	30.4
Waypoint 7	17.6	7.3	55.0	30.8
Waypoint 8	26.2	12.9	39.4	22.0
Waypoint 9	13.1	0.5	50.7	29.9
Waypoint 10	5.2	0.1	39.1	5.0
HAMO-2	--	--	5.9	14.1 <sup>†</sup>

\* Based on orbit determination reconstruction, with uncertainty below 50 m and 1 cm/s  $1\sigma$ .  
<sup>†</sup> Cancelled maneuver – deviation was determined to be acceptable.

Figure 16 shows the evolution of the reconstructed spacecraft position and velocity during the executed maneuvers (the sole cancelled maneuver is not included) compared to the corresponding 10 maneuver designs targeting each of the LAMO to HAMO-2 Waypoints. Note that the maneuver starting at Waypoint 9 was targeting Waypoint 10, but due to a lack of deterministic thrusting before Waypoint 10, was also targeting HAMO-2. The final maneuver, between Waypoint 10 and HAMO-2, was determined to be unnecessary and cancelled. The result is that the error in delivery to Waypoint 10 continued to grow uncorrected to HAMO-2.



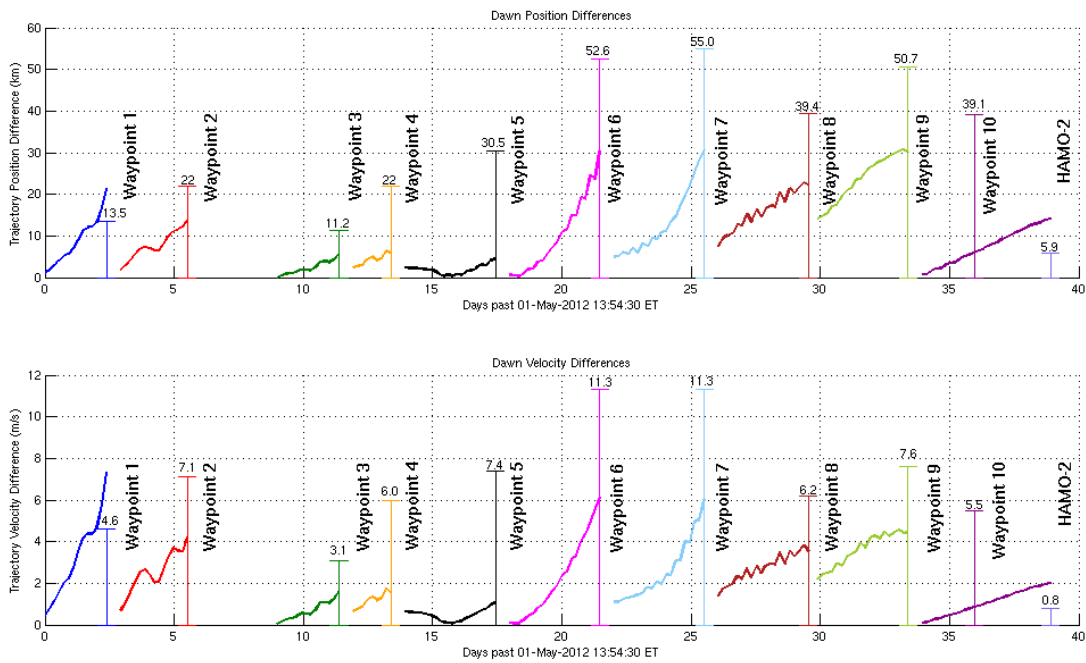


**Figure 16 - LAMO to HAMO-2 Maneuver Design Trajectories versus Reconstructed Transfer Trajectory**

The comparison between the reference trajectory designed to be flown, and the reconstructed trajectory actually flown, is shown in Figure 17. The differences shown illustrate how far the spacecraft deviated from the reference trajectory between Waypoints. The largest difference exceeds 400 km from the reference trajectory, an intentional deviation needed to satisfy attitude control constraints.

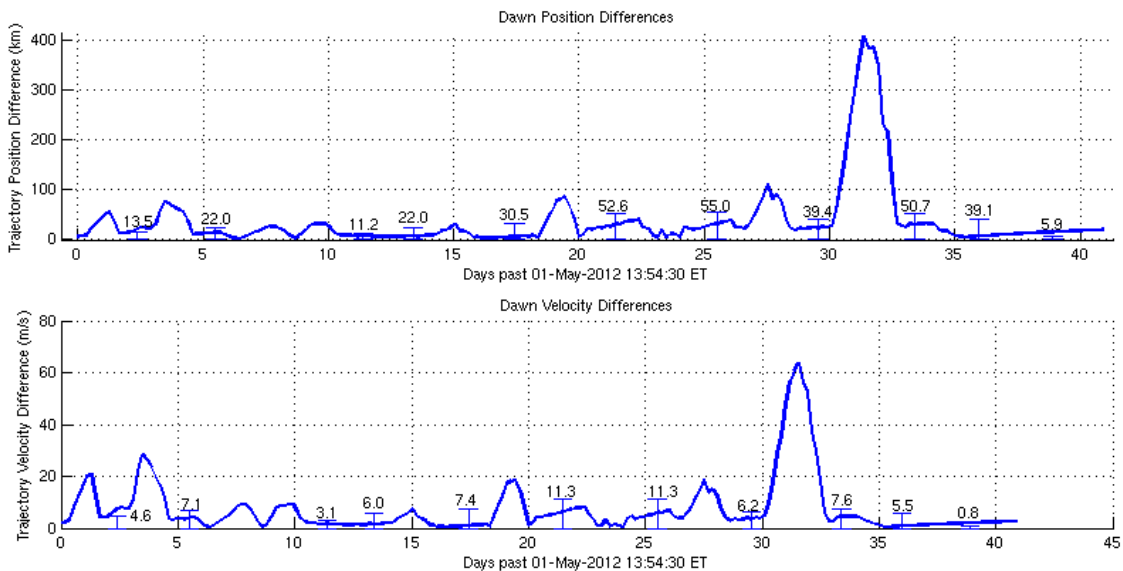


**Figure 17 - LAMO to HAMO-2 Reference Trajectory versus Reconstructed Transfer Trajectory**

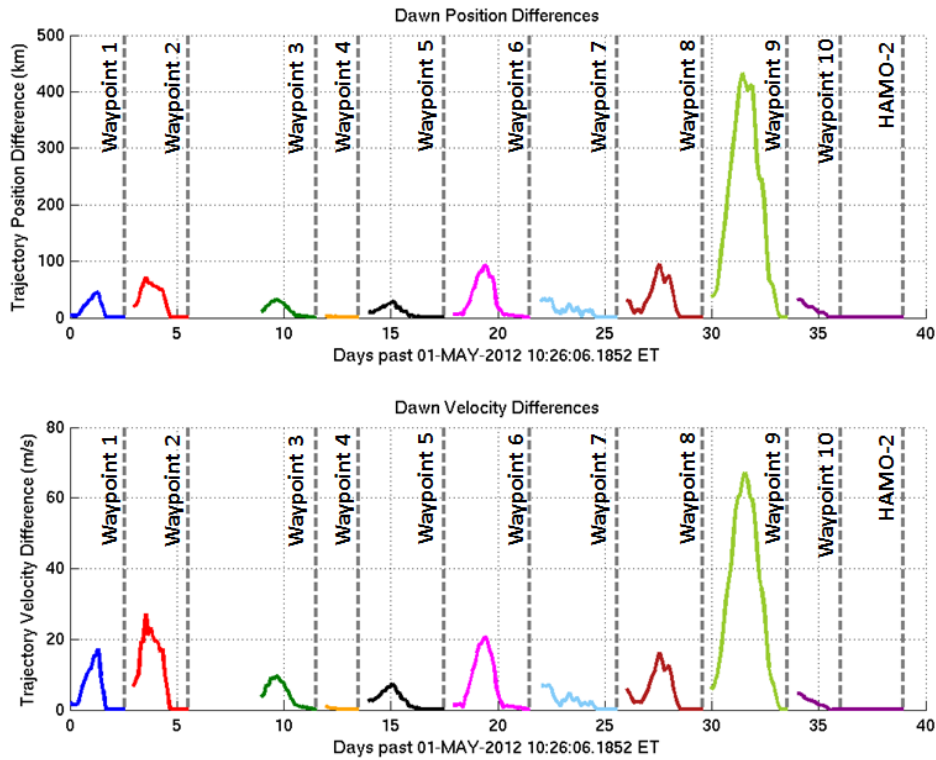


**Figure 18 - LAMO to HAMO-2 Maneuver Design Trajectories versus Reference Trajectory**

Figure 18 illustrates the difference between each of the 10 designed maneuvers and the reference trajectory. The largest intentional deviation from the reference trajectory occurs between Waypoints 8 and 9, where attitude control constraints were particularly challenging. This maneuver heavily employed thrust direction optimization, sending the spacecraft far from the reference before returning to the reference trajectory at the next Waypoint. A similar, more benign effect can be seen in many of the other maneuvers which move farther from the reference trajectory than the initial state. Due to the large excursion between Waypoints 8 and 9, the maneuver design trajectory was re-evaluated for favorable powered-flight stability<sup>20</sup> characteristics and was found to be comparable to the reference trajectory.

Finally, Figure 19 includes the spacecraft telemetry-based determination of angular thrust delivery error for each of the designed maneuvers during the transfer. The Veil Monte Carlo analysis used to develop the navigation plan for this transfer<sup>10</sup> assumed that the spacecraft would suffer more than 1 degree of pointing error at all times, more than 3 degrees of pointing error for just over 10% of the each maneuver, and occasional deviations of more than 10 degrees. By comparison, 76% of the values shown in Figure 19 are less than 1 degree, only 0.9% exceed 3 degrees, and none exceed 5 degrees.

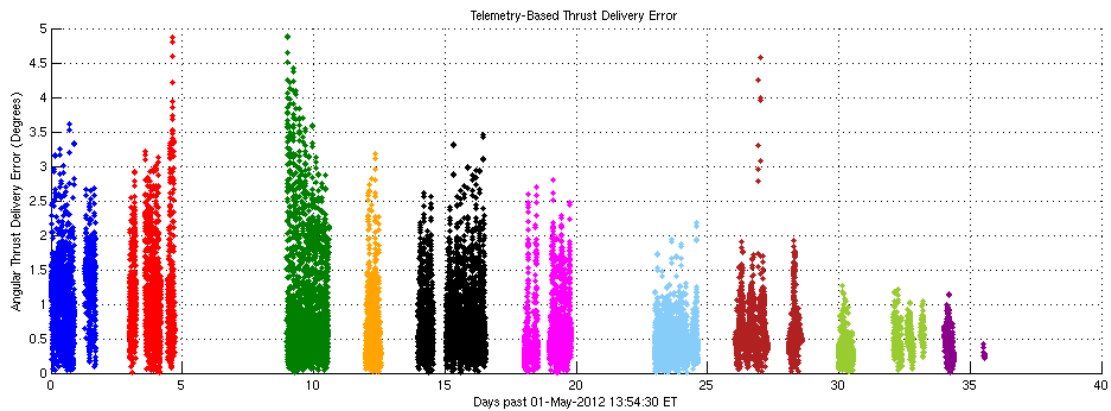


**Figure 19 - LAMO to HAMO-2 Predicted Attitude Control Thrust Delivery Errors**

## CONCLUSIONS

Delivery to each of the transfer Waypoints was more accurate than anticipated by the Monte Carlo analysis used to develop the transfers in almost all cases. This is largely due to conservative maneuver execution error assumptions. Maneuver execution error models were most conservative for maintenance maneuvers during LAMO where maneuvers were designed in inertially fixed directions, mitigating angular thrust delivery error. The ability to perform small maneuvers in inertially fixed directions, the use of direction optimization to reduce angular thrust delivery errors, and the ability to design a reference trajectory that avoids thrust directions known to increase thrust delivery error should all be considered when formulating execution error models.

Deviations from the reference trajectory due to attitude control requirements on maneuver pointing were larger than anticipated, and, in one case, warranted powered flight stability analysis on the maneuver trajectory due to the spacecraft distance from the stable reference trajectory. Future low thrust missions relying on specific reference trajectory characteristics and employing thrust direction optimization to meet thrust direction constraints should consider the deviation between Waypoints introduced by direction optimization.

## ACKNOWLEDGEMENTS

Special thanks go to the Dawn Attitude Control Subsystem team and Marc Rayman for assistance in development of maneuver execution error models. This work was performed at the Jet Propulsion Laboratory, California Institute of Technology, under a contract with the National Aeronautics and Space Administration. Copyright 2013 California Institute of Technology. Government sponsorship acknowledged.

## REFERENCES

- <sup>1</sup> Russel, C.T. *et al.*, "Dawn: A journey in space and time", *Planetary and Space Science*, Vol. 52, Issues 5-6, Apr.-May 2004, pp. 465-489.
- <sup>2</sup> Rayman, M.D. *et al.*, "Dawn: A mission in development for exploration of main belt asteroids Vesta and Ceres", *Acta Astronautica*, Vol. 58, Issue 11, June 2006, pp. 605-616.
- <sup>3</sup> Rayman, M.D., and Patel, K.C., "The Dawn project's transition to mission operations: On its way to rendezvous with (4) Vesta and (1) Ceres", *Acta Astronautica*, Vol. 66, Issues 1-2, Jan.-Feb. 2010, pp. 230-238.
- <sup>4</sup> De Sanctis, M.C. *et al.*, "Spectroscopic Characterization of Mineralogy and Its Diversity Across Vesta", *Science*, vol. 336, May. 2012, pp. 697-700.

- <sup>5</sup> Jaumann, R. *et al.*, “Vesta’s Shape and Morphology”, *Science*, vol. 336, May. 2012, pp. 687 – 690.
- <sup>6</sup> Reddy, V. *et al.*, “Color and Albedo Heterogeneity of Vesta from Dawn”, *Science*, vol. 336, May. 2012, pp. 700 – 704.
- <sup>7</sup> Russell, C. T. *et al.*, “Dawn at Vesta: Testing the Protoplanetary Paradigm”, *Science*, vol. 336, May. 2012, pp. 684 – 686.
- <sup>8</sup> Schenk, P. *et al.*, “The Geologically Recent Giant Impact Basins at Vesta’s South Pole”, *Science*, vol. 336, May. 2012, pp. 694 –697.
- <sup>9</sup> Marchi, S. *et al.*, “A Violent Collisional History of Asteroid 4 Vesta”, *Science*, vol. 336, May. 2012, pp. 690 –694.
- <sup>10</sup> Parcher, D.W., and Whiffen, G.J., "Dawn Statistical Maneuver Design for Vesta Operations", Paper AAS 2011-180, 21<sup>st</sup> AAS/AIAA Space Flight Mechanics Meeting, New Orleans, Louisiana, Feb. 13-17, 2011.
- <sup>11</sup> Parcher, D.W., "Low-Thrust Orbit Transfer Design for Dawn Operations at Vesta", Paper AAS 2011-183, 21<sup>st</sup> AAS/AIAA Space Flight Mechanics Meeting, New Orleans, Louisiana, Feb. 13-17, 2011.
- <sup>12</sup> Whiffen, G.J., "Low Altitude Mapping Orbit Design and Maintenance for the Dawn Discovery Mission at Vesta", Paper AAS 2011-182, 21<sup>st</sup> AAS/AIAA Space Flight Mechanics Meeting, New Orleans, Louisiana, Feb. 13-17, 2011.
- <sup>13</sup> Han, D., “Orbit Transfers for Dawn’s Vesta Operations: Navigation and Mission Design Experience”, 23rd International Symposium on Space Flight Dynamics, Pasadena, California, Oct. 29 – Nov. 2, 2012.
- <sup>14</sup> Whiffen, G.J., "Static/Dynamic Control for Optimizing a Useful Objective," United States Patent No. 6,496,741, Issued Dec. 17, 2002, Filed Mar. 25, 1999.
- <sup>15</sup> Whiffen, G.J., and Sims, J.A., "Application of SDC Optimal Control Algorithm to Low-Thrust Escape and Capture Including Fourth Body Effects," 2nd International Symposium on Low Thrust Trajectories, Toulouse, France, June 18-20, 2002.
- <sup>16</sup> Whiffen, G.J., "Mystic: Implementation of the Static Dynamic Optimal Control Algorithm for High-Fidelity, Low-Thrust Trajectory Design", Paper AIAA 2006-6741, AIAA/AAS Astrodynamics Specialist Conference, Keystone, Colorado, Aug. 21-24, 2006.
- <sup>17</sup> Abrahamson, M. *et al.*, “Dawn Orbit Determination Team: Trajectory Modeling and Reconstruction Process at Vesta”, Paper AAS 2013-346, 23<sup>rd</sup> AAS/AIAA Space Flight Mechanics Meeting, Kauai, Hawaii, Feb. 10-14. 2013.
- <sup>18</sup> Whiffen, G.J., "Thrust Direction Optimization: Satisfying Dawn's Attitude Agility Constraints", Paper AAS 2013-343, 23<sup>rd</sup> AAS/AIAA Space Flight Mechanics Meeting, Kauai, Hawaii, Feb. 10-14. 2013.
- <sup>19</sup> Smith, J.C. *et al.*, “Spiraling Away from Vesta: Design of the Transfer from Low to High Altitude Mapping Orbits”, Paper AAS 2013-350, 23<sup>rd</sup> AAS/AIAA Space Flight Mechanics Meeting, Kauai, Hawaii, Feb. 10-14. 2013.
- <sup>20</sup> Whiffen, G.J., "The Stability of Powered Flight Around Asteroids With Application to Vesta", Paper AAS 2011-186, 21<sup>st</sup> AAS/AIAA Space Flight Mechanics Meeting, New Orleans, Louisiana, Feb. 13-17 2011.